第22卷第3期
2003年6月

红外与毫米波学报
J. Infrared Millim. Waves

Vol. 22, No. 3
June, 2003

TWO-DIMENSIONAL INFRARED CORRELATION SPECTROSCOPY STUDIES OF PROTEINS IN AQUEOUS SOLUTIONS

WU Yuqing[1)] Ozaki Yukihiro[2)]

([1)] Key Laboratory for Supramolecular Structure and Materials of the Ministry of Education, Jilin University, Jilin, Changchun 130023, China;

[2)] Department of Chemistry, School of Science and Technology, Kwansei-Gakuin University, Sanda, Hyogo 669-1337, Japan)

Abstract This review paper aims at outlining the principle of two-dimensional (2D) IR spectroscopy and its applications to the subtle structural changes of proteins in aqueous solutions. Our studies have dual purposes. One is to show that 2D ATR/IR spectroscopy can be utilized to explore the effects of adsorption of proteins on an ATR cell. Another purpose is to provide new insight into temperature and acid induced protein structure and denaturation by using 2D IR spectroscopy.

Key words two-dimensional correlation spectroscopy, protein, structural changes, infrared spectroscopy(IR).

二维相关红外光谱研究溶液中蛋白质的结构

吴玉清[1)] 尾崎幸洋[2)]

([1)] 吉林大学超分子结构与材料教育部重点实验室, 吉林, 长春, 130023;

[2)] Department of Chemistry, School of Science and Technology, Kwansei-Gakuin University, Sanda, Hyogo 669-1337, Japan)

摘要 概述了二维相关红外光谱基本原理以及它在研究蛋白质结构变化方面的最新应用,所综述的内容主要包括以下几个方面:(1)二维相关掠角反射红外光谱研究蛋白质分子在样品池上的吸附过程;(2)重点概述二维相关红外光谱在研究温度、酸度等物理变量诱导蛋白质变性及结构变化方面的应用.

关键词 二维相关光谱,蛋白质,结构变化,红外光谱.

INTRODUCTION

Fourier transform infrared spectroscopy (FT-IR) has been used extensively as a powerful technique for exploring the secondary structures of proteins.[1~5] By using FT-IR one can investigate the secondary structures even for proteins with huge molecular weight. It is also of note that IR spectroscopy allows one compare the secondary structure of proteins among aqueous solutions, solids, and crystals. In the IR region, the frequencies of bands due to the amide Ⅰ, Ⅱ, and Ⅲ vibrations are sensitive to the secondary structure elements of proteins.[1~5] Usually, second derivative, Fourier self deconvolution (FSD) and curve fitting are used to deconvolute the amide Ⅰ band. However, the results obtained by the above methods are not always conclusive, especially for complex proteins consisting of various secondary structures.

In recent years generalized two-dimensional (2D) correlation spectroscopy[6,7] has been introduced as a new technique for analyzing amide Ⅰ, Ⅱ and Ⅲ bands of proteins.[8~16] 2D IR correlation spectroscopy

* The project Supported by a Grant-in-Aid to Y. Ozoki(No. 11640516), the Major State Research Development Program of NSFC (No. G2000078102) and project of NSFC(No. 20003004)
Received 2002 - 02 - 26, revised 2003 - 02 - 20

* 日本文部省尾崎幸洋专项基金(批准号 11640516),国家重点基础研究发展规划项目(批准号 G2000078100)和自然科学基金委(批准号 20003004)资助项目
稿件收到日期 2002 - 02 - 26, 修改稿收到日期 2003 - 02 - 20

is very useful for protein research because of three major reasons. One is that 2D correlation spectroscopy enables one to deconvolute the amide bands into component bands due to different secondary structures. Another is that it allows establish the correlation between different secondary structures of protein through selective correlation peaks for a given perturbation. Yet another is that it gives information about specific order of secondary structural changes and changes in amino acid residues under various environments.

This review paper aims at outlining the principle of 2D IR spectroscopy and its applications to the structural and dynamics studies of proteins in aqueous solutions. It consists of two parts; the first part deals with the mathematical background and important properties of 2D IR. The advantages of 2D IR correlation analysis for protein research are also discussed in the first part. In the second part of this review, our recent studies on applications of 2D IR to proteins are described. Our studies have dual purposes. One is to develop 2D IR spectroscopy as powerful methods for investigating proteins in aqueous solutions. It was also shown that 2D ATR/IR spectroscopy can be utilized to explore the effects of adsorption of proteins on an ATR cell.[13] Another purpose of our studies is to provide new insight into protein structures and denaturation by using 2D IR spectroscopy. We have been particularly interested in protein denaturation by temperature[17], acid[15], and concentration[13].

1 Principles of 2D Correlation Spectroscopy

Fig. 1 illustrates the basic scheme for a 2D correlation spectroscopy experiment based on an external perturbation. The general experimental approach used in 2D correlation spectroscopy is based on the detection of dynamic variations of spectroscopic signals induced by an external perturbation.[6,7,18] Thus, for example, one can employ temperature-dependent IR spectra, pH-dependent NIR spectra, concentration dependent Raman spectra, and so on for obtaining 2D correlation spectra.[19,20]

The mathematical background for 2D correlation spectroscopy has been described in detail by Noda.[6,7] Briefly, the following procedures are applied to obtain 2D correlation spectra. Let us consider a series of time-dependent spectra. First, a series of dynamic spectra $\tilde{y}(v,t)$ must be calculated by subtracting a reference spectrum $\bar{y}(v)$ from each spectrum obtained.

$$\tilde{y}(v,t) = \begin{cases} y(v,t) - \bar{y}(v) & for\ -T_{min}/2 \leqslant t \leqslant T_{max}/2 \\ 0 & otherwise \end{cases} . \tag{1}$$

Where $\bar{y}(v)$ is the reference spectrum. The selection of the reference spectrum is somewhat arbitrary, but it is usually set to be the static or time-averaged spectrum defined as

$$\bar{y}(v) = \frac{1}{T_{max} - T_{min}} \int_{T_{min}}^{Tmax} y(v,t)\,dt. \tag{2}$$

For the next step, it is necessary to Fourier transform the dynamic spectra measured in the time domain into the frequency domain. The dynamic spectra are then discreted Fourier transform to $\tilde{Y}_1(\omega)$.

$$\begin{aligned} \tilde{Y}_1(\omega) &= \int_{-\infty}^{\infty} \tilde{y}(v_1,t) e^{-i\omega t} dt \\ &= \tilde{Y}_1^{Re}(\omega) + i\tilde{Y}_1^{Im}(\omega) \end{aligned} \tag{3}$$

Where $\tilde{Y}_1^{Re}(\omega)$ and $\tilde{Y}_2^{Im}(\omega)$ are the real and imaginary components of the complex Fourier transform of $\tilde{y}(v_1,t)$. The Fourier frequency ω represents the individual frequency component of the time-dependent variation of $\tilde{y}(v_1,t)$. Similarly, $\tilde{Y}_2(\omega)$, the conjugate of the Fourier transform of dynamic spectral intensity $\tilde{y}(v_2,t)$ at spectral variable v_2, is given by Eq. (4):

$$\begin{aligned} \tilde{Y}_2^{*}(\omega) &= \int_{-\infty}^{\infty} \tilde{y}(v_2,t) e^{+i\omega t} dt \\ &= \tilde{Y}_2^{Re}(\omega) - i\tilde{Y}_2^{Im}(\omega). \end{aligned} \tag{4}$$

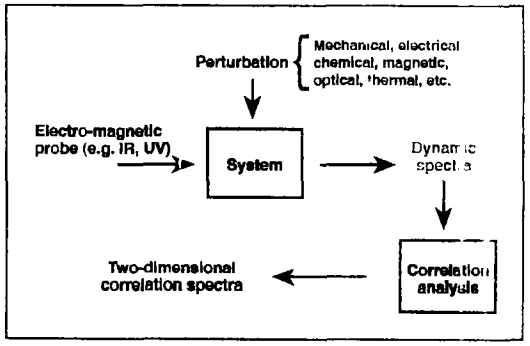

Fig. 1 General scheme for obtaining 2D correlation spectra (Reproduced from Ref. [7] with permission. Copyright © 2000, Society for Applied Spectroscopy.)
图 1 获取二维相关光谱图的一般示意图(摘自文献[7],版权© 2000,应用光谱学会)

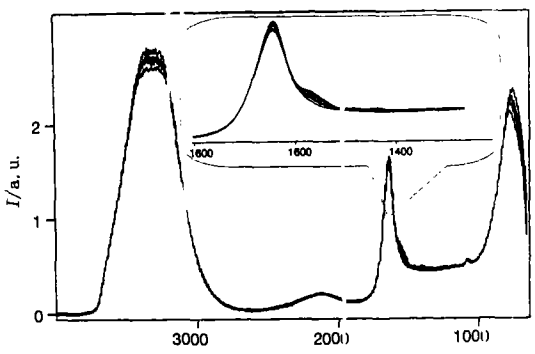

Fig. 2　ATR/IR spectra of the buffer solution and five kinds of aqueous solutions of BLG with concentrations of 1,2,3,4, and 5 wt% (Reproduced from Ref. [13] with permission. Copyright © 2000, American Chemical Society.)

图 2　乳球蛋白缓冲溶液的衰减全反射红外光谱图,溶液中乳球蛋白的质量百分比浓度分别为 1,2,3,4,5%(摘自文献[13],版权© 2000,美国化学学会)

Now, one can define the complex 2D correlation intensity between $\tilde{y}(v_1,t)$ and $\tilde{y}(v_2,t)$. 2D correlation is nothing but a quantitative comparison of spectral intensity variations observed at two different spectral variables over some finite observation interval between T_{min} and T_{max} Eq. (5) yields the complex 2D correlation intensity.

$$\Phi(v_1,v_2)+i\Psi(v_1,v_2)=\frac{1}{\pi(T_{max}-T_{min})}\int_0^{\infty}\tilde{Y}_1(\omega)\tilde{Y}_2^*(\omega)\,d\omega \qquad (5)$$

Where $\Phi(v_1,v_2)$ and $\Psi(v_1,v_2)$ are called the synchronous and asynchronous intensities, respectively. The synchronous 2D correlation spectra represent the simultaneous or coincidental changes of spectral intensity variations measured at v_1 and v_2 during the interval between T_{min} and T_{max}, while the asynchronous 2D correlation spectra represents sequential, or successive, changes of spectral intensities.

2　Application of 2D IR Correlation Spectroscopy to Proteins

Recently, generalized 2D IR correlation spectroscopy has been extensively used to investigate the conformational changes of proteins.[8~15,16,19,20] For example Nabet and Pezolet[8] clearly showed the potential of 2D IR correlation spectroscopy in probing the conformation of proteins using H-D exchange. Smeller and Heremans[9], and Dzwolak et al.[10] reported 2D IR studies of pressure-dependent structural modifications of proteins. Paquet et al.[11] employed 2D IR spectroscopy to investigate the aggregation of cytochrome *c* in the presence of dimyristoylphophatidylglycerol. There are many other examples.[12~15,16,19,20] In this section we introduce two examples of 2D IR studies form our recent research.[13,15]

2.1　2D ATR/IR correlation spectroscopy studies of concentration-dependent spectral variations of β-lactoglobulin in aqueous solutions.

Fig. 2 displays ATR/IR spectra in the 4000-650cm^{-1} region of BLG solutions with a concentration of 1,2,3,4, and 5wt% and phosphate buffer solution (pH 6.6).[13] As expected, the spectra are almost featureless and very colse to an ATR/IR spectrum of water. To pick out subtle changes in spectral intensities from the stack of raw spectral traces, the original spectra were subjected to pretreatment procedures consisting of ATR correction, subtraction of the spectrum of the buffer solution, and smoothing.[13] Fig. 3 shows the resulting spectra of the protein solutions after the four pretreatments expect for the normalization.[13] One can clearly identify amide Ⅰ, Ⅱ, and Ⅲ bands in the regions of 1690 ~ 1620, 1570 ~ 1520, and 1320 ~ 1220 cm^{-1}, respectively. Czarnik-Matusewicz et al[13] examined both adsorption-induced and concentration-dependent spectral variations of BLG using 2D ATR/IR correlation spectroscopy. It was found from the ad-

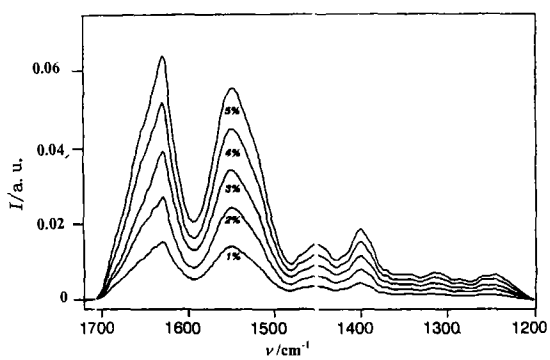

Fig. 3　Concentration-dependent ATR/IR spectral variations of the BLG solutions after four kinds of pretreatments, except for normalization. (Reproduced from Ref. [13] with permission. Copyright © 2000, American Chemical Society.)

图 3　不同浓度的乳球蛋白溶液的衰减全反射红外差减光谱图;对应浓度分别为 1,2,3,4,5%.(摘自文献[13],版权© 2000,美国化学学会)

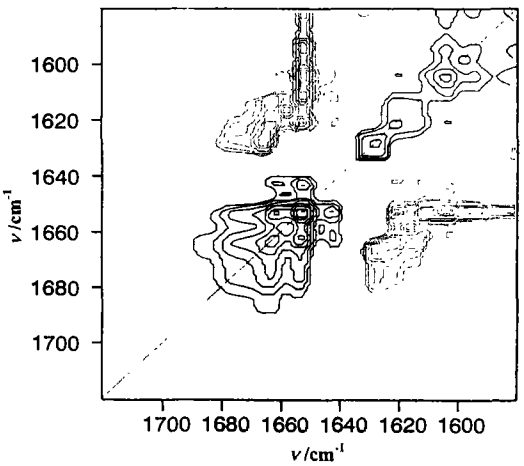

Fig. 4 Synchronous 2D ATR/IR correlation spectrum region constructed from concentration-dependent spectral changes of BLG (Reproduced from Ref. [13] with permission. Copyright © 2000, American Chemical Society.)
图 4 以浓度为变量的乳球蛋白溶液的二维同步相关红外光谱图(摘自文献[13],版权© 2000,美国化学学会)

sorption-dependent spectral variations that the interaction between BLG molecules and an ATR prism is characterized by intensity changes in bands assigned to β-sheet elements buried in the hydrophobic core of the molecule and that the intensity variations induced by the adsorption are about one-tenth of those induced by the concentration changes. In this review only the concentration-dependent structural changes in BLG are discussed.

Fig. 4 depicts the synchronous 2D ATR/IR correlation map obtained from concentration-dependent spectral changes of the BLG aqueous solutions. The strongest autopeaks are developed at 1652 and 1662cm^{-1}. These peaks are assigned to hydrophilic secondary structure motives located on the outer surface of BLG that are build from α-helices and 3_{10}-helices. These secondary structures are less protected from water penetration than the β-strands forming the calyx. A minimal intensity variation in the band at 1636cm^{-1} due to antiparallel "buried" β-sheets is consistent with the fact that the C = O groups located inside the hydrophobic core of BLG are more resistant to the interaction with water molecules than those in the hydrophilic, solvent exposed part of BLG. This 2D result leads to the conclusion that the C = O groups in the β-sheets are less accessible to water molecules than those in the α-helical fragments.

Fig. 5 depicts the corresponding asynchronous correlation spectrum and Fig. 6 shows a slice spectrum extracted at 1665cm^{-1} from the asynchronous 2D spectrum in Fig. 5, together with that at 1640cm^{-1} from the asynchronous spectrum calculated from the adsorption-dependent spectral changes. Comparison between the two slice spectra shows that the unrelated intensity variations stimulated by concentration change are at least one order of magnitude higher than those induced by the adsorption process. According to the rule proposed by Noda,[6,7] the asynchronous spectrum in Fig. 5 and the slice spectrum at 1665cm^{-1} in Fig. 6 suggest the following sequence of the spectral events occurring during the concentration changes:

$$(1645 \approx 1642) \rightarrow (1694 \approx 1683 \approx 1658 \approx 1654) \rightarrow (1673 \approx 1665) \rightarrow (1638 \approx 1633 \approx 1628) \rightarrow 1623 \rightarrow 1616 \rightarrow 1606\text{cm}^{-1}$$

concentration

The above sequence reveals that the first event in the intensity variations occur for the bands due to the random coil structure, followed by the intensity changes in the bands assigned to the high-wavenumber β-sheet component (1694cm^{-1}), β-turn (1683cm^{-1}), and α-helix (1658 and 1654cm^{-1}). The intensity variations arising from another type of β-turn (probably type Ⅲ) (1673cm^{-1}) and 3_{10} helix (1665cm^{-1}) take place next. The intensity modifications attributed to both "exposed" β-strands ("buried" (1638cm^{-1}), 1633, and 1628cm^{-1}) are behind those due to the structures described above, but ahead the changes induced by aggregated components (1623cm^{-1}). The last event in the sequence is attributed to the side-chain vibrations (1616, 1606cm^{-1}).

2.2 2D ATR/IR correlation spectroscopy study of pH-dependent changes in the secondary structures and hydrogen bonding of carboxylic groups of human serum albumin

It is well known that HSA molecule undergoes several transitions under acidic and basic conditions, assuming *E* from (below pH 2.7), *F* form (pH 2.7 ~ 4.3), *N* form (pH 4.3 ~ 8.0), *B* form (pH 8.0 ~

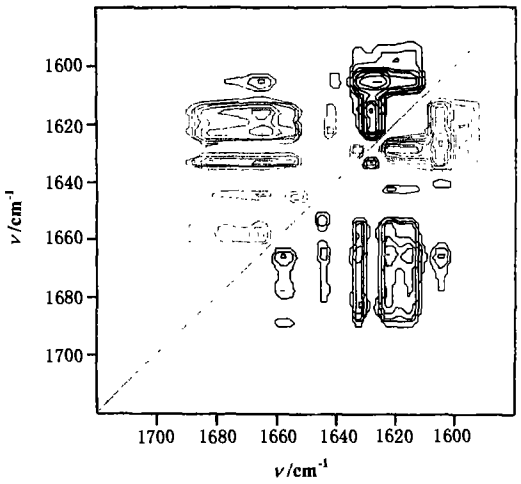

Fig. 5　Asynchronous 2D ATR/IR correlation spectrum in the 1720 ~ 1580cm^{-1} region constructed from concentration-dependent spectral changes of BLG (Reproduced from Ref. [13] with permission. Copyright © 2000, American Chemical Society.)

图 5　以浓度为变量的乳球蛋白溶液的二维非同步相关红外光谱图,光谱范围为 1720 ~ 1580 波数(摘自文献[13],版权© 2000,美国化学学会)

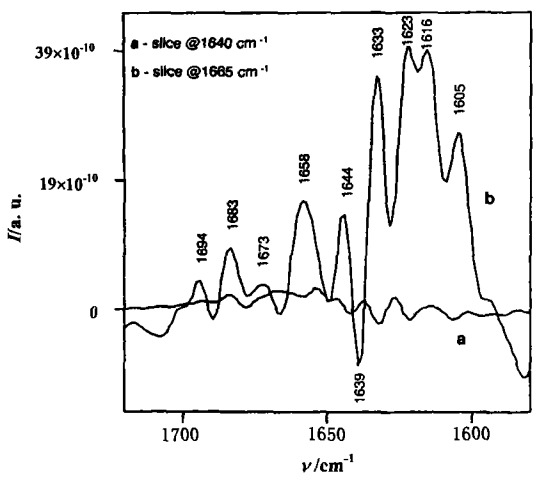

Fig. 6　Slice spectra extracted along (a) 1640cm^{-1} in the asynchronous spectrum generated from the adsorption-dependent spectral variations and (b) 1665cm^{-1} in the asynchronous spectrum presented in Fig. 5 (Reproduced from Ref. [13] with permission. Copyright © 2000, American Chemical Society.)

图 6　(a)以浓度为变量的乳球蛋白溶液的二维同步相关光谱在 1640 波数处的切面图;(b)以浓度为变量的乳球蛋白的二维非同步相关光谱在 1665 波数处的切面图.(摘自文献[13],版权© 2000,美国化学学会)

10) and *A* form (over pH10).[22~26] The acid-induced structural modifications of HSA are characterized by changes in secondary as well as tertiary structures and microenvironmental changes in side chains. The acid-induced transitions in bovine serum albumin (BSA) and HSA have been investigated extensively by use of a variety of methods, but there are still many things to be explored as to the secondary structural changes, roles in microenvironmental changes in side chains, and functions of the three domains. Murayama et al.[15] employed 2D IR correlation spectroscopy to investigate pH-dependent alterations in the backbone conformations and hydrogen bonding of side chains, particularly of COOH and COO$^-$ groups of glutamic (Glu) and aspartic (Asp) acid residues and relation between the changes in the secondary structures and the hydrogen bonds.

Fig. 7 displays difference ATR/IR spectra in the 1750 ~ 1580cm^{-1} region of the HSA solutions (2.0 wt%) with pH of 3.2, 3.6, 4.2, 4.6 and 5.0 (the spectrum of buffer solution at each pH was already subtracted).[15]

Fig. 8a and Fig. 8b show synchronous and asynchronous 2D IR correlation spectra of the *N* isomeric form of HSA in the buffer solutions, generated from the pH-dependent (pH 5.0, 4.8, 4.6 and 4.4) spectral changes in the 1750 ~ 1580cm^{-1} region.[15] The synchronous correlation map develops only a prominent autopeak near 1654cm^{-1}. This autopeak is largely due to the amide I band of the α-helix structures of HSA.

In contrast to the synchronous spectrum the asynchronous spectrum shows a number of cross peaks. The analysis of cross peaks identifies bands at least at 1715, 1667, 1654, 1641, and 1614cm^{-1}. Of note is an appearance of a broad feature around 1715cm^{-1} assignable to a C = O stretching mode of the hydrogen bonded COOH groups of Glu and Asp residues of HSA. This band is not identified in the second derivative spectra at pH 5.0 and pH 4.6. Thus, the clear observation of the band at 1715cm^{-1} demonstrates the usefulness of 2D correlation spectroscopy. It was reported that about half of the carboxyls of Asp and Glu residues are ionized with an intrinsic p*K* of 4.3[22] Therefore, it seems that some carboxylate groups undergo protonation even in this pH range (pH 5.0 ~ 4.4), yielding the C = O stretching mode of the COOH groups at 1715 cm^{-1}.

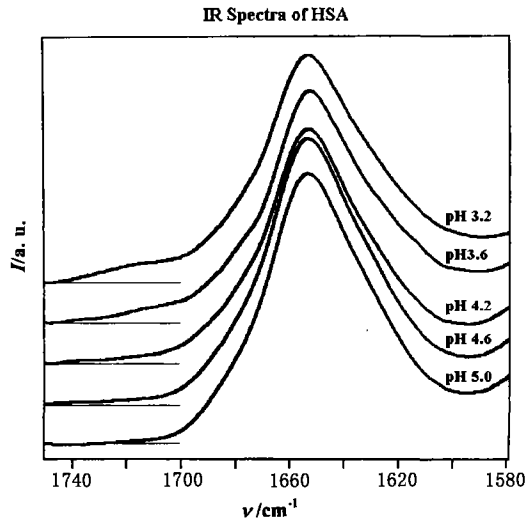

Fig. 7 Representative difference IR spectra of HSA in buffer solutions (2.0 wt%) of pH3.2, 3.6, 4.2, 4.6 and 5.0. At each pH the spectrum of the buffer solution was subracted from the corresponding spectrum of the HSA solution. (Reproduced from Ref. [15] with permission. Copyright © 2001, American Chemical Society.)
图7 人血清白蛋白溶液在不同 pH 值缓冲溶液中的红外差减光谱图,对应 pH 值分别为3.2, 3.6, 4.2, 4.6, 5.0;(摘自文献[15],版权© 2000,美国化学学会)

HSA contains 36 Asp and 62 Glu residues, and thus, it is very important to investigate the protonation and hydrogen bonds of the carboxyls.

Based on the signs of asynchronous cross peaks, Murayama et al. [15] discussed the sequence of band intensity changes;

Hydrogen-bonded COOH (1715cm^{-1}), side chains (1614cm^{-1})

→ α-helix (1654cm^{-1}) → β-strand (1641cm^{-1}) → β-turn (1667cm^{-1})

It seems in the N form that the protonation of the COO^- groups and microenvironmental changes in the side chains precede the secondary structural changes, which begin with the α-helices, followed by β-strands, and β-turns. The above sequence implies that the protonation of some carboxylic groups at relatively high pH (4.5 ~ 5.0) is a trigger for the secondary structural changes in the N form.

Fig. 9(a) and Fig. 9(b) depict the synchronous and asynchronous correlation maps of the N-F transition, respectively, generated from the IR spectra of HSA solutions of pH 4.6, 4.4, 4.2, 4.0 and 3.8. [15] An interesting point in the synchronous map is appearances of negative cross peaks at (1705, 1632) cm^{-1} and (1705, 1640) cm^{-1}. The bands at 1740 and 1705cm^{-1} are assigned to a C = O stretching vibration of free and hydrogen bonded COOH groups, respectively, of Asp and Glu of HSA. In this pH range, many carboxylic groups are protonated. It is very likely that the unfolding or expansion of domain Ⅲ induces the free COOH groups in the N-F transition. The band at 1705cm^{-1} due to the hydrogen bonded COOH group and that at 1632cm^{-1} assignable to β-strand structures

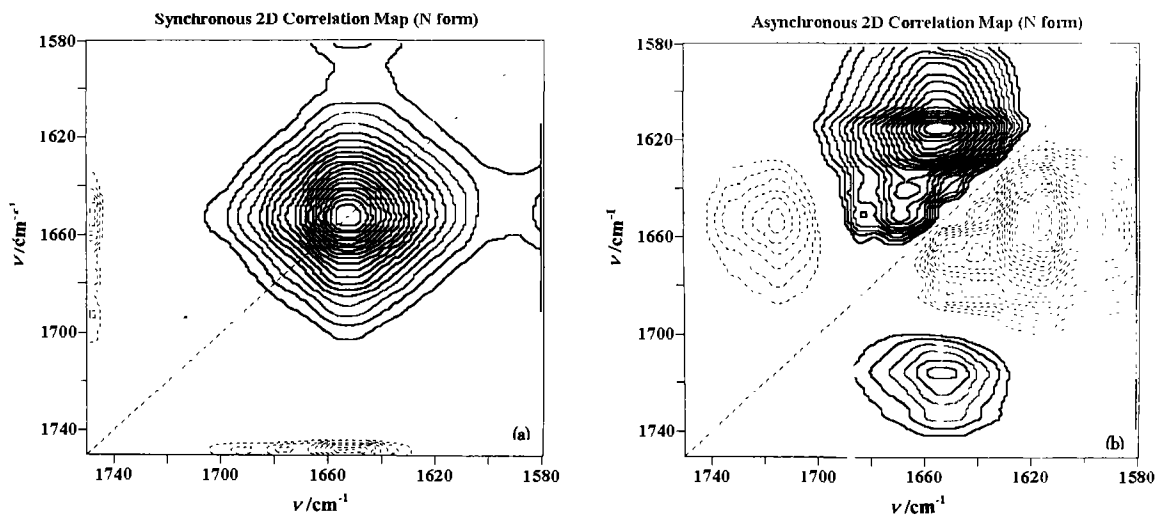

Fig. 8 (a) Synchronous 2D IR correlation spectrum constructed from the pH-dependent (pH 5.0, 4.8, 4.6 and 4.4) spectral variations of the HSA solutions with a concentration of 2.0 wt%. (b) The corresponding asynchronous 2D IR correlation spectrum. (Reproduced from Ref. [15] with permission. Copyright © 2001, American Chemical Society.)
图8 以浓度为变量的乳球蛋白溶液的二维同步相关红外光谱图.(摘自文献[15],版权© 2001,美国化学学会)

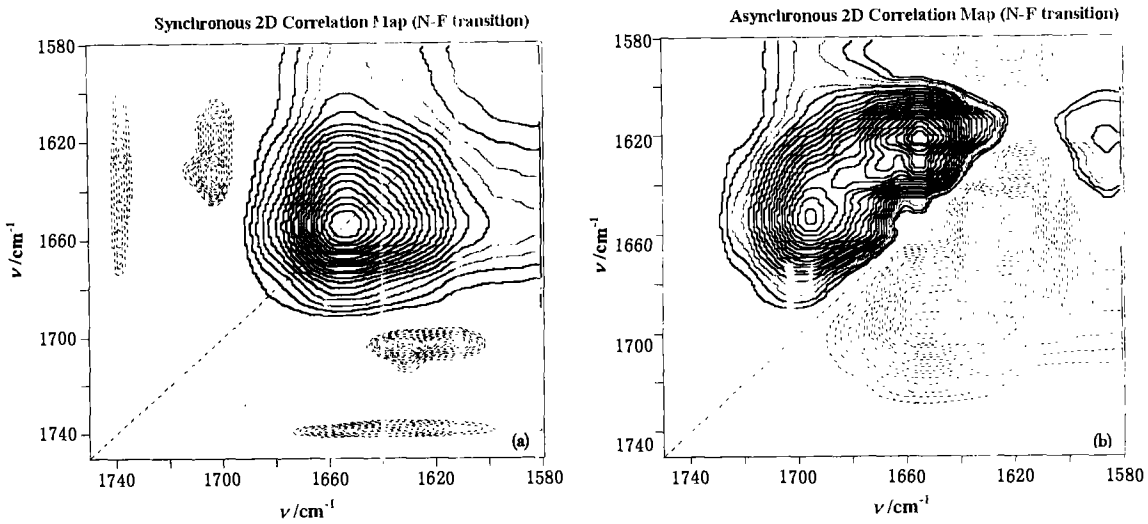

Fig. 9　(a) Synchronous 2D IR correlation spectrum constructed from the pH-dependent (pH 4.6, 4.4, 4.2, 4.0 and 3.8) spectral variations of the HSA solutions with a concentration of 2.0 wt%. (b) The corresponding asynchronous 2D IR correlation spectrum. (Reproduced from Ref. [15] with permission. Copyright © 2001, American Chemical Society.)
图 9　以酸度为变量的二维相关红外光谱图,对应 pH 值分别为 4.6, 4.4, 4.2, 4.0, 3.8;(a)同步相关红外光谱图;(b)非同步相关红外光谱图. (摘自文献[15],版权© 2001,美国化学学会)

share the cross peak, suggesting that the formation of the hydrogen bonded COOH groups upon the protonation and the conformational change in β-strand structures are cooperative in the N-F transition. Moreover, the long cross peak between the band at 1740cm^{-1} and other bands indicates that both the α-helix and β-strand structures change in-phase with the formation of the free COOH groups.

The asynchronous spectrum (Fig. 9b) develops cross peaks at (1696, 1654) and (1620, 1654) cm^{-1}. The bands at 1696, 1654, and 1620cm^{-1} may be due to hydrogen bonded COOH groups, α-helices, and β-sheets, respectively. It is noted that there are two kinds of hydrogen bonded COOH groups in the N-F transition that show the C = O stretching mode at 1705 and 1696cm^{-1}. The C = O groups can form hydrogen bonds with NH groups of the main chains or side chains or with OH groups of side chains or water molecules. Therefore, the C = O stretching bands of the hydrogen-bonded COOH groups appear in a rather wide range.

The close inspection of the signs of the asynchronous cross peaks in Fig. 9b suggests the following sequence of the structural changes in HSA during the N-F transition.

Hydrogen-honded COOH (1696cm^{-1}) → α-helix (1654cm^{-1})

→β-sheet (1620cm^{-1}), β-turn (1667cm^{-1}) → β-strand (1632cm^{-1})

Therefore, it seems that the protonation of COO^- groups starts the N-F transition, followed by the unfolding of the α-helices in domain Ⅲ. In the last step, the β-turns, β-sheets, and β-strands undergo the secondary structure changes, leading to the Fisomeric form of HSA. Both in the N isomeric form and in the N-F transition, the formation of hydrogen bonded COOH groups upon the protonation of COO^- groups induces the conformational changes of HSA. However, one must notice that the COOH groups with the stronger hydrogen bonds are formed in the N-F transition; the bands due to the COOH groups appear at 1715cm^{-1} in the N form but they appear at 1705 and 1696cm^{-1} in the N-F transition. Besides the 2D IR study by Murayama et al.,[15] there are much evidence showing that the protonation of carboxylate groups plays a key role in the initiation of the N-F transition.[25] Most of the evidences come from the Trp and Tyr Fluorescence studies.

In this way the acidic unfolding process of HSA was investigated by generalized 2D ATR/IR correlation spectroscopy. The 2D correlation spectra provided information not only about the secondary structure variations but also about the changes in the COO^- and

COOH groups and other side chains. This is unique advantage of 2D IR correlation spectroscopy in protein research.

REFERENCES

[1] Clark R J H, Hester R E, eds. *Biomolecular Spectroscopy*. Chichester: John Wiley & Sons, 1993, **20**: Part A, **21**: Part B

[2] Havel H A. *Spectroscopic Methods for Determining Protein Structure in Solution*. Chichester: John Wiley & Sons, 1995

[3] Jackson M, Mantsch H H. The use and misuse of FTIR spectroscopy in the determination of protein structure. *Critical Rev. Biochem. Mol. Biol.*, 1995, **30**: 95

[4] Torii H, Tasumi M. In: *Infrared Spectroscopy of Biomolecules*. Mantsch H H, Chapman D, eds. New York: John Wiley & Sons, 1996: 1

[5] Haris P I, Chapman D. *Infrared Spectroscopy of Biomolecules*. New York: John Wiley & Sons, 1996: 239

[6] Noda I. Generalized two-dimensional correlation method applicable to infrared, Raman, and other types of spectroscopy. *Appl. Spectrosc*, 1993, **47**: 550

[7] Noda, I. Determination of two-dimensional correlation spectra using the hilbert transform. *Appl. Spectrosc*, 2000, **54**: 994

[8] Nabet A, Pezolet M. Two-dimensional FTIR spectroscopy: a powerful method to study the secondary structure of proteins using H-D exchange. *Appl. Spectrosc*, 1997, **51**: 466

[9] Swellers L, Heremans K. 2D FT-IR spectroscopy analysis of the pressure-induced changes in proteins. *Vib. Spectrosc.*, 1999, **19**: 375

[10] Dzwolak W, Kato M, Shimizu A, *et al*. Comparative two-dimensional fourier transform infrared correlation spectroscopic study on the spontaneous pressure-and temperature-enhanced H/D exchange in α-lactalbumin. *Appl. Spectrosc.*, 2000, **54**: 963

[11] Paquet M J, Auger M, Pezolet M. 2D-IR study of the aggregation of lipid-bound cytochrome c. Ozaki Y, Noda I, eds. *AIP Conference Proceedings*. New York: American Institute of Physics, 2000, **503**: 103

[12] Schultz C P, Fabian H, Mantsch H H. Two-dimensional mid-IR and near-IR correlation spectra of ribonuclease A: using overtones and combination modes to monitor changes in secondary structure. *Biospectrosc.*, 1998, **4**: S19

[13] Czarnik-Matusewicz B, Murayama K, Wu Y, *et al*. Two-dimensional attenuated total reflection/infrared correlation spectroscopy of adsorption-induced and concentration-dependent spectral variations of β-lactoglobulin in aqueous solutions. *J. Phys. Chem. B*, 2000, **104**: 7803

[14] Wu Y, Murayama K, Ozaki Y. Two-dimensional infrared spectroscopy and principal component analysis studies of the secondary structure and kinetics of hydrogen-deuterium exchange of human serum albumin. *J. Phys. Chem. B*, 2001, **105**: 6251

[15] Murayama K, Wu Y, Czarnik-Matusewicz B, *et al*. Two-dimensional/attenuated total reflection infrared correlation spectroscopy studies on secondary structural changes in human serum albumin in aqueous solutions: pH-dependent structural changes in the secondary structures and in the hydrogen bondings of side chains. *J. Phys. Chem. B*, 2001, **105**: 4763

[16] Jung Y M, Czarnik-Matusewicz B, Ozaki Y. Two-dimensional infrared, two-dimensional Raman, and two-dimensional infrared and Raman heterospectral correlation studies of secondary structure of β-lactoglobulin in buffer solutions. *J. Phys. Chem. B*, 2000, **104**: 7812

[17] Wu Y, Czarnik-Matusewicz B, Murayama K, *et al*. Two-dimensional near-infrared spectroscopy study of human serum albumin in aqueous solutions: using overtones and combination modes to monitor temperature-dependent changes in the secondary structure. *J. Phys. Chem. B*, 2000, **104**: 5840

[18] Wu Y, Jiang J, Ozaki Y. A New Possibility of Generalized Two-Dimensional Correlation Spectroscopy: Hybrid Two-Dimensional Correlation Spectroscopy. *J. Phys. Chem.* A, 2002, **106**: 2422.

[19] Ozaki Y, Noda I, eds. Two-dimensional correlation spectroscopy. *AIP Conference Proceedings*. New York: American Institute of Physics, 2000: 503

[20] Wu Y, Murayamak, Czarnik-Matusewicz B, *et al*. Two-dimensional/attenuated total reflection/infrared correlation spectroscopy studies on concentration and heat-induced structural changes of human serum albumin in aqueous solutions. *Appl. Spectrosc*, 2002, **56**: 1186

[21] Crowfoot D M, Riley D P. Structure of β-lactoglobulin. *Nature*, 1938, **141**: 521

[22] Peters T Jr. *All About Albumin, Biochemistry, Genetics, and Medical Applications*. New York: Academic Press, 1994: 35

[23] Protein Data Bank, Department of Chemistry, Brookhaven National Laboratory, Upton, NY 11973, USA, HTTP://WWW.RCSB.ORG/PDP/. Structure Explore-1A06

[24] Carter D C, Ho J X. Structure of serum albumin. *Adv. Protein Chem.*, 1994, **45**: 153

[25] Era S, Sogami M. H-NMR and CD studies on the structural transition of serum albumin in the acidic region——the N→F transition. *J. Pept. Res.*, 1998, **52**: 431